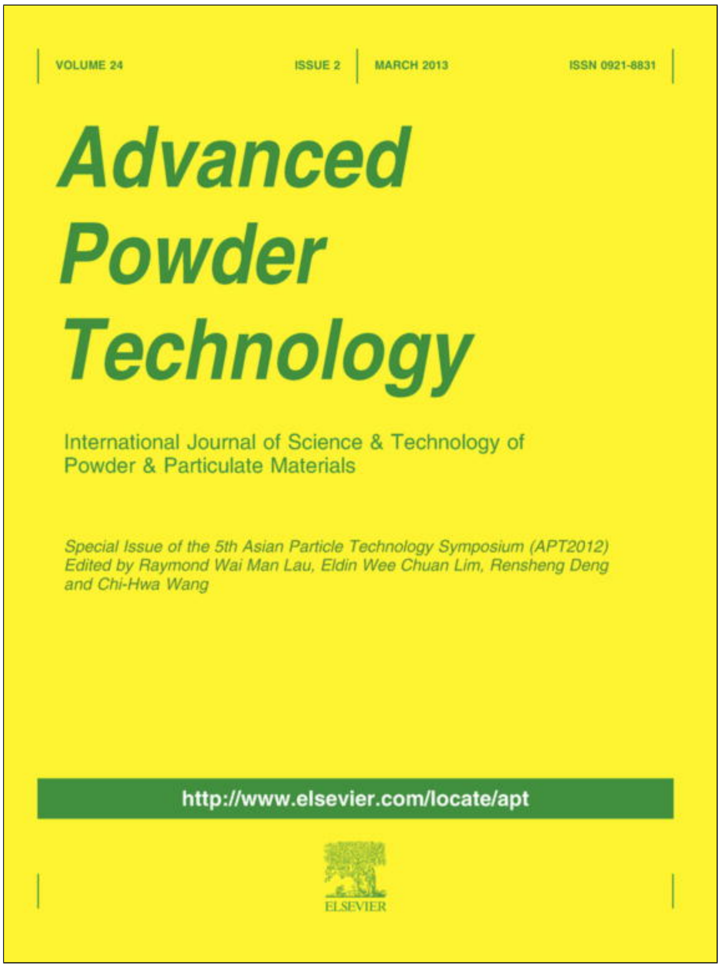

VOLUME 24 | ISSUE 2 | MARCH 2013 | ISSN 0921-8831

Advanced Powder Technology

International Journal of Science & Technology of Powder & Particulate Materials

Special Issue of the 5th Asian Particle Technology Symposium (APT2012)
Edited by Raymond Wai Man Lau, Eldin Wee Chuan Lim, Rensheng Deng and Chi-Hwa Wang

http://www.elsevier.com/locate/apt

ELSEVIER

Advanced Powder Technology 24 (2013) 549–553

Contents lists available at SciVerse ScienceDirect

Advanced Powder Technology

journal homepage: www.elsevier.com/locate/apt

Original Research Paper

The novel, one step and facile synthesis of ZnO nanoparticles using heteropolyoxometalates and their photoluminescence behavior

Hamed Rashidi[a], Ali Ahmadpour[a,*], Fatemeh F. Bamoharram[b], Majid M. Heravi[c], Ali Ayati[a]

[a] *Department of Chemical Engineering, Ferdowsi University of Mashhad, Mashhad, Iran*
[b] *Department of Chemistry, Mashhad Branch-Islamic Azad University, Mashhad, Iran*
[c] *Department of Chemistry, School of Sciences, Alzahra University, Tehran, Iran*

ARTICLE INFO

Article history:
Received 21 April 2012
Received in revised form 19 September 2012
Accepted 24 October 2012
Available online 22 November 2012

Keywords:
ZnO
Nanoparticles
Heteropolyoxometalate
Wet chemical method
Photoluminescence

ABSTRACT

A novel and facile wet chemical method is presented to synthesize zinc oxide nanoparticles (NPs) under ambient atmosphere and temperature. Keggin type heteropolyoxometalate ($H_3[PW_{12}O_{40}]$) was used as stabilizer and the effect of stirring time and amount of $H_3[PW_{12}O_{40}]$ (HPW) were studied. XRD and TEM techniques were applied for the morphological and structural characterizations of NPs. Size of nanoparticles were determined using TEM, Scherrer's formula as well as effective mass approximation. The results of these three methods are in good agreements and revealed single hexagonal zincite type crystalline with average particle size in the range of 3–15 nm. Photoluminescence behavior of the prepared sample shows a strong orange to red emission centred at about 620–635 nm, a green emission at around 550 nm and broad UV emission at around 400 nm.

1. Introduction

Zinc oxide is an important semiconductor with a relatively high excitation binding energy (60 meV) and a wide direct band gap (3.37 eV). The tailoring of this metal oxide to the desired shape has attracted extensive attention, due to its various shape-induced functions. This high excitation binding energy allows excitonic transitions at room temperature, leading to high radiative recombination efficiency for spontaneous emission as well as lower threshold voltage for emission. Zinc oxide NPs (NPs) have received wide attention due to their specific chemical, electrical, surface and microstructural properties. These nanoparticles with the features of large volume to surface area ratio, high ultraviolet absorption and long life-span [1] proved to have greater potential for being used as gas sensor [2], solar cell [1], photocatalyst degradation [3,4] relative to TiO_2 NPs [5]. They have also been employed as efficient catalysts for liquid phase hydrogenation [6], chemical absorbent [7], and UV absorber in cosmetics and anti-virus agent [8]. The physical and microstructural properties of ZnO can be modified by changing the synthetic method [9,10].

ZnO NPs can be synthesized via various methods such as sol–gel processing [11,12], mechanical milling [13], homogeneous precipitation [14], spray pyrolysis [15], organometallic synthesis [16], thermal decomposition of organic precursors [17], supercritical-water processing [18], RF plasma synthesis [19], direct precipitation [20], vapor transport process [21], self assembling [22], microemulsion synthesis [23], microwave irradiation [24], hydrothermal processing [25], thermal evaporation [26], mechanochemical synthesis [27], and wet chemical methods [28–31]. Regarding these versatile applications and having various preparation methods in hand, introduction of the new and more facial synthetic routes and as well as modification on nanosized ZnO with new techniques are still in much demands.

Polyoxometalates (POMs) are a class of inorganic metal–oxygen cluster compounds with unique molecular structure, chemical characters and electronic versatility [32]. Previously, most studies on POMs were mainly focused on their catalytic and photochemical properties [33–35]. Several properties of POMs such as simultaneous stabilization and reduction ability, designate them as suitable reagents for the synthesis of NPs, have been recently reported [36–38]. It is known that by changing the pH and temperature of the environment, the structure, size, and stability of the colloidal nanoparticles can be changed [39]. We have come to the conclusion that ZnO NPs are stabilized by HPW. However, this phenomenon is rather complex. It is suggested that different factors such as number of protons, spherical structure and bronsted acidity of HPW, as well as pH are significantly determinative. The external circumstances such as additives and solvent composition can also be effective [40].

In this study, a novel method to synthesize zinc oxide nanoparticles with wet chemical method under ambient atmosphere and

---

* Corresponding author. Tel./fax: +98 511 8816840.
E-mail address: ahmadpour@um.ac.ir (A. Ahmadpour).

0921-8831/$ - see front matter © 2012 The Society of Powder Technology Japan. Published by Elsevier B.V. and The Society of Powder Technology Japan. All rights reserved.
http://dx.doi.org/10.1016/j.apt.2012.10.008

temperature, using the tungstophosphoric acid (HPW) as the most famous and important types of POMs, as stabilizer, is presented. We believe this method is well worthwhile being considered as a promising option for the large scale production of ZnO NPs.

2. Experimental

2.1. Synthesis methodology

Zinc acetate dehydrate ($Zn(Ac)_2{\cdot}2H_2O$), Dimethylsulfoxide (DMSO), Ethanol (analytical grade), Potassium hydroxide (KOH), and Keggin type heteropolyacid ($H_3[PW_{12}O_{40}]$) were purchased from Merck KGA and used as received. Zinc acetate dihydrate solution (0.2 M) was dissolved in 20 mL DMSO under vigorous stirring to form a clear solution. A solution of KOH (1.2 M) in 10 mL ethanol was then added to the above solution drop wise under moderate stirring condition until it becomes uniformly white. In each experiment, the required amounts of $H_3[PW_{12}O_{40}]$ (HPW) was added and stirring time was continued for mixing the stabilizer thoroughly. The white precipitates were separated, using centrifugation technique and then washed several times with DI water and ethanol, respectively, to remove all impurities and then dried at 60 °C for 8 h. The dried synthesized ZnO NPs were used for further characterizations.

2.2. Measurements and analysis

The morphology of the prepared nanoparticles was determined by transmission electron microscope (TEM, LEO-912AB) with an acceleration voltage of 120 kV. Copper mesh was used for TEM analysis.

Analysis of crystal structure and crystal size has been carried out by X-ray diffraction. The prepared ZnO NPs were characterized by X-ray diffraction (XRD) (Bruker D8 Advance) using Cu Kα radiation ($\lambda = 1.5406$ Å). The size of crystals was calculated via Scherrer's formula using full-width at half-maximum (FWHM) of XRD patterns [41]:

$$D = \frac{0.9\ \lambda}{\beta\ \cos\theta} \tag{1}$$

where λ is wave length of X-ray source, β is FWHM in radians, and θ is Bragg's diffraction angle.

UV–vis absorption study has been performed using Avantes Avaspec-3648 single beam spectrophotometer. Methanol was used for dispersing zinc oxide NPs. Size of NPs can be calculated by converting the energy corresponding to the excitation absorption peak in terms of particle size using the effective mass approximation [42]:

$$E = E_g + h^2\pi^2\left(\frac{1}{m_e}+\frac{1}{m_h}\right) - \frac{(1.8e^2)}{4\pi\varepsilon'\varepsilon'_0 R} + \text{Smaller term} \tag{2}$$

where E is band gap of synthesized particles, E_g is bulk band gap of ZnO (3.3 eV), R is radius of the particle, m_e is effective mass of electron ($0.28m_o$), m_h is effective mass of the hole ($0.49m_o$), ε' is dielectric constant of material (9.1), ε'_0 is permittivity of free space, and h is Planck's constant.

Photoluminescence (PL) evaluation has been done at room temperature, using Perkin Elmer (LS-45) Luminescence Spectrophotometer.

3. Results and discussion

Prior to discuss the parameters in preparation of ZnO NPs, it is preferred to consider their morphology and crystal structure. Fig. 1 shows the XRD pattern of prepared samples at different stirring times with 0.2 g HPW. These peaks at scattering angles (2θ) correspond to the reflection from: 100, 002, 101, 102, 110, 103, and 112 crystal planes. Hence, one can conclude they possess a hexagonal zincite type crystalline.

The expanded peaks in XRD pattern indicate ultra-fine nature of the crystallites. The average crystal sizes estimated from Scherrer's formula using FWHM are in the range of 3–6 nm. From Fig. 1, it is clear, with proceeding the stirring time from 30 min to 1 h, the peaks become sharper, indicating the complete formation of crystal structure. It is also worthwhile to mention that there are no distinct changes observed with further increasing the stirring time from 1 to 9 h.

3.1. Effect of HPW amount

To investigate, the effect of HPW amount, a series of experiments was performed at 1 h stirring. Fig. 2 shows the UV–vis absorption spectra of the prepared samples with different amounts of HPW.

From Fig. 2 it can be seen that there is a gradual "blue shift" in the UV absorption spectra with increasing the HPW amount, indicating that the size of ZnO NPs have been decreased. Fig. 3 also shows variation of UV absorption peak with different amounts of HPW.

From the mass approximation using Eq. (2), the corresponding size of NPs can be obtained. Table 1 shows the evaluated sizes.

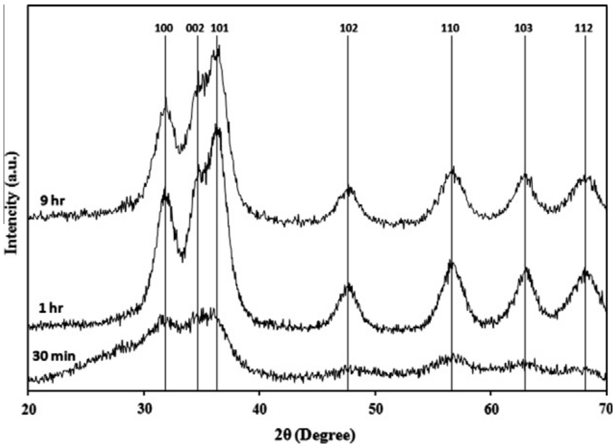

Fig. 1. XRD pattern of ZnO nanoparticles prepared at different stirring times.

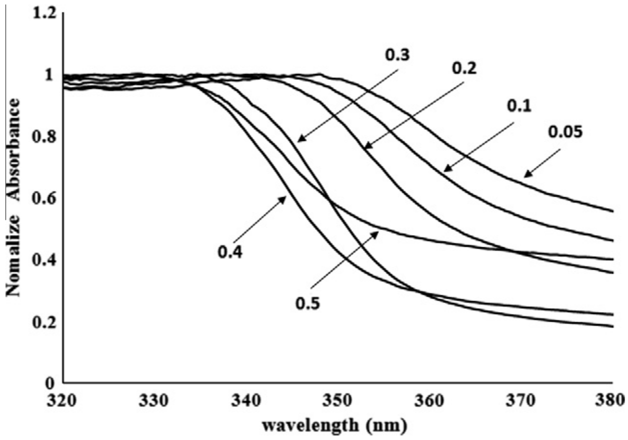

Fig. 2. Effect of HPW amount on UV–vis absorption spectra of prepared samples.

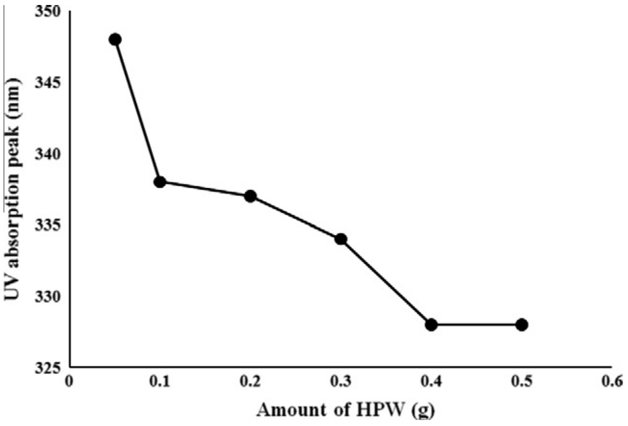

Fig. 3. Variation of UV absorption peak with the amount of HPW.

Table 1
Approximate size of ZnO nanoparticles obtained from the mass approximation.

HPW amount (g)	UV absorption peak (nm)	Approximate size of NPs (nm)
0.05	348	15–20
0.1	338	3–4
0.2	337	3–4
0.3	334	~3
0.4	328	<3
0.5	328	<3

With respect to Fig. 3 and Table 1, it can be seen that with increasing the amount of HPW up to 0.4 g, the size of NPs are decreased and further increase in the amount of HPW becomes ineffective.

3.2. TEM analysis

Fig. 4 provides representative TEM images of the ZnO NPs synthesized with 0.4 g HPW at 1 h stirring time. Although the particles are agglomerated, which is due to the lack of any stabilizing surfactants in the present method, they are almost distinguishable from each other. Formation of Zn–O–Zn bonds among NPs, due to the existence of water molecules, leads to hard agglomeration that restricts the applications of ZnO NPs. It is found that for reducing hard agglomeration of particles, removal of water in the precursors is a key process that can be done using various methods [43]. For successful applications of nanomaterials and to enhance surface chemical and physical properties, coating of nanoparticles is also the key technological route.

From Fig. 4, we can see that, the produced NPs exhibits almost uniform size and spherical morphology with an average diameter of about 5 nm, which is in good agreement with the results of UV–vis absorption spectra.

3.3. FTIR spectra

The FTIR spectrum of the synthesized ZnO powders (Fig. 5) showed main absorption bands assigned for the O–H stretching of hydroxyl group at about 3422 cm^{-1} and Zn–O stretching bond at about 450 cm^{-1}.

The peak at 1629 cm^{-1} is attributed to H–O–H bending vibration, which is caused by small amount of water existing in the final product. The peaks at 1085, 950 and 828 cm^{-1} are respectively assigned to an inner P–O$_a$–W bond, an external W = O$_c$ bond and W–O$_b$–W bridges (where O$_a$ is the oxygen in P–O tetrahedron, O$_b$ is the bridging oxygen of two octahedral sharing a corner, and O$_c$ is the bridging oxygen of two octahedral sharing an edge), indicating the presence of HPW on the surface of ZnO NPs. However, no diffraction peaks of HPW can be detected in XRD pattern of the ZnO powders (Fig. 1), which may be due to the very small amounts of HPW adsorbed on the surface of the prepared ZnO powders [44]. The stability of the structure of HPW in the reaction mixture has been checked by FTIR spectroscopy. At the end of the reaction, FTIR spectrum of reaction mixture (Fig. 6) showed all of the characteristic bonds of HPW as described above. Note that, in Fig. 6, the peaks at 1584, 1400, 1338 and 620 cm^{-1} are attributed to the DMSO which was removed after several washing (Fig. 5).

3.4. Photoluminescence properties

Fig. 7 shows a room temperature PL spectrum of the ZnO sample prepared using 0.4 g HPW for 1 h stirring, excited at 350 nm. Since this sample had the smallest particle size among the other samples, only, its PL spectrum is reported. From Fig. 7, a strong orange to red emission is centred at about 620–635 nm. This strong emission may be caused by the surface/interface defects in the structure of ZnO NPs due to combination of deeply trapped holes to shallowly trapped electrons [45] or zinc anti-sites and oxygen [29]. The UV near band edge emission at around 390 nm (UV emission), which attributed to free excitation recombination, is not clearly observed in this PL spectra and only a broad and weak peak is observed in this region. The broad PL peak at around 400 nm is attributed to zinc vacancies [29]. This assignment has also been reported previously [46,47]. Many types of

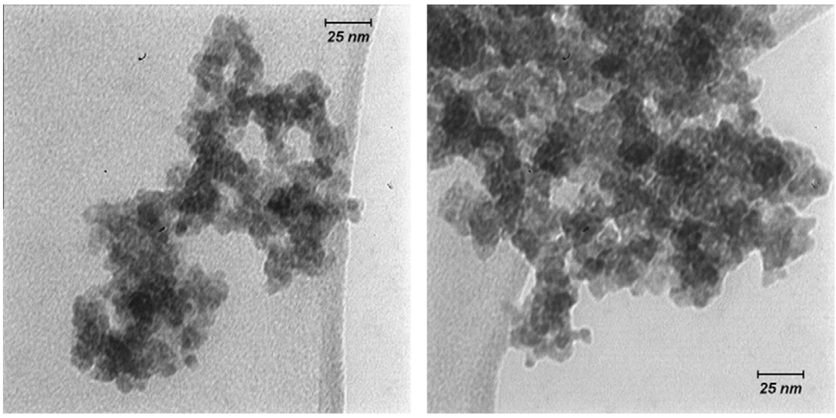

Fig. 4. TEM images of prepared ZnO NPs with 0.4 g of HPW at 1 h stirring time.

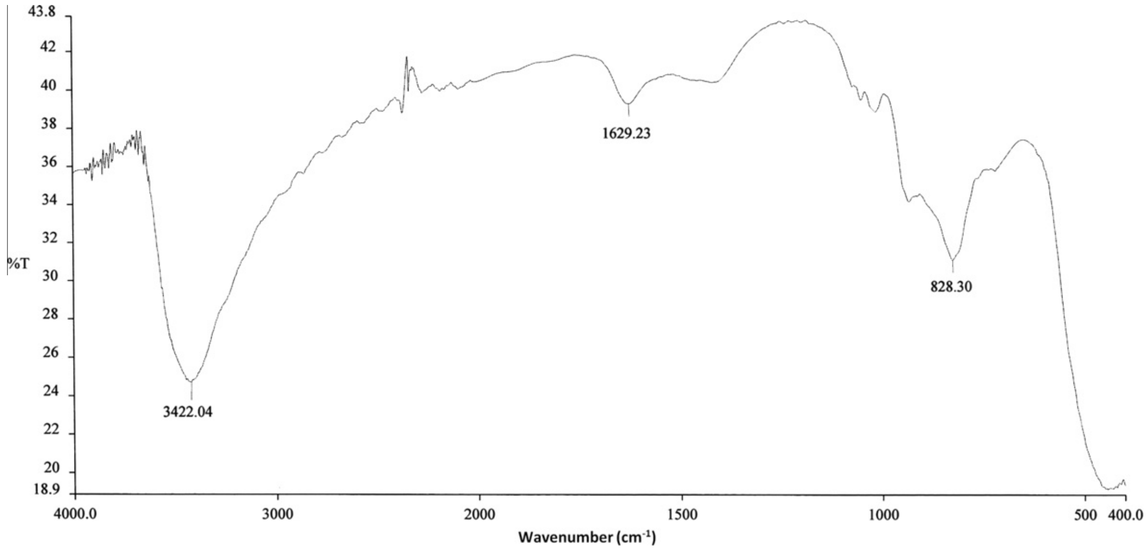

Fig. 5. FT-IR spectrum of prepared ZnO NPs with 0.4 g of HPW at 1 h stirring time.

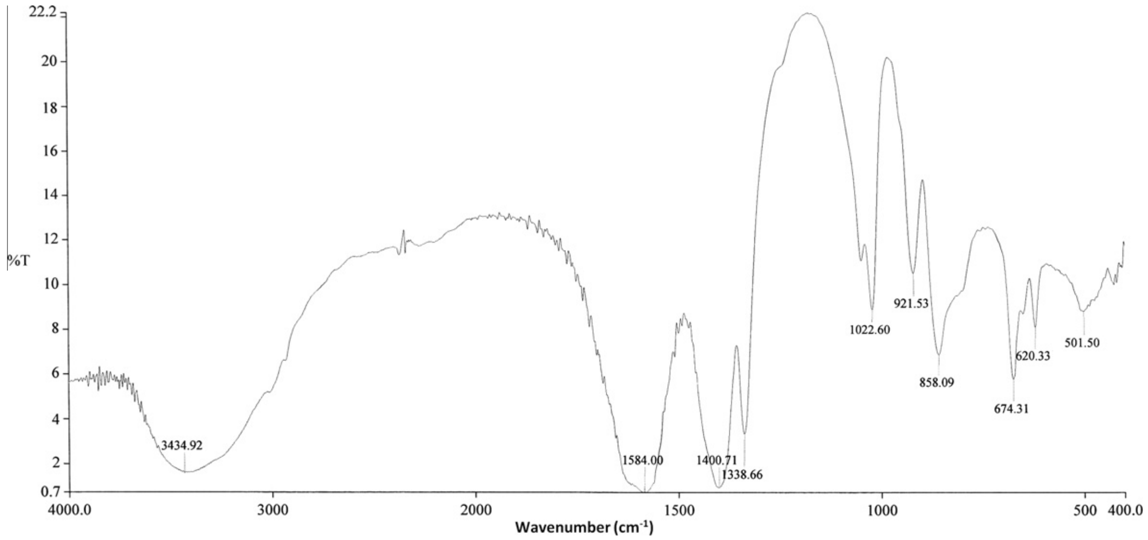

Fig. 6. FT-IR spectrum of the reaction mixture before washing.

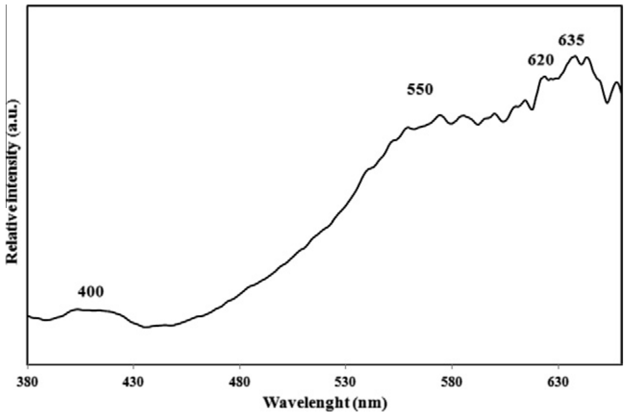

Fig. 7. Room temperature PL spectrum of the sample prepared with 0.4 g of HPW at 1 h stirring time.

intrinsic and extrinsic defects with different ionization states could be responsible for the visible PL in ZnO NPs [45].

A green emission at around 550 nm is also observed which is known to be a deep level emission caused by impurities, oxygen vacancies and the structural defects in the crystals such as zinc interstitials [48]. The green band emission corresponds to the singly ionized oxygen vacancy in ZnO and excess oxygen on the surface of these NPs, which might be in the form of OH^- ions resulting from the recombination of photo-generated hole with single ionized charge state of this defect is also noticed. The weak green emission also implies that there are few surface defects in ZnO nanoparticles [29].

4. Conclusion

A novel, rapid and facile wet chemical method has been presented to synthesize zinc oxide NPs by using HPW as a stabilizer. It was found that HPW is an effective stabilizer for the purpose. The effect of HPW amounts was also studied. XRD and TEM of NPs were used for morphological and structural characterizations. Size of nanoparticles was determined using TEM, Scherrer's formula and effective mass approximation. The results of three different techniques show that the average sizes of NPs are in the range of 3–15 nm. Photoluminescence behavior of the prepared sample show a strong orange to red emission centred at about 620–635 nm, a green emission at around 550 nm, and the broad UV emission at around 400 nm which is attributed to free excitation recombination.

References

[1] D. Yu, R. Cai, Z. Liu, Catalytic synthesis and structural characteristics of high-quality tetrapod-like ZnO nanocrystals by a modified vapor transport process, Spectrochim. Acta Part A 60 (2004) 1617.

[2] J. Xu, Q. Pan, Y.A. Shun, Z. Tian, Grain size control and gas sensing properties of ZnO gas sensor, Sens. Actuators B 66 (2000) 277.

[3] M.L. Curridal, R. Comparelli, P.D. Cozzli, G. Mascolo, A. Agostiano, Colloidal oxide nanoparticles for the photocatalytic degradation of organic dye, Mater. Sci. Eng. C 23 (2003) 285.

[4] V.P. Kamat, R. Huehn, R. Nicolaescu, A “sense and shoot” approach for photocatalytic degradation of organic contaminants in water, J. Phys. Chem. B 106 (2002) 788.

[5] R. Hong, Z. Ren, J. Ding, H. Li, Experimental investigation and particle dynamic simulation for synthesizing titania nanoparticles using diffusion flame, Chem. Eng. J. 108 (2005) 203.

[6] G.M. Hamminga, G. Mul, J.A. Moulijn, Real-time in situ ATR-FTIR analysis of the liquid phase hydrogenation of -butyrolactone over Cu–ZnO catalysts: a mechanistic study by varying lactone ring size, Chem. Eng. Sci. 59 (2004) 5479.

[7] R. Turton, D.A. Berry, T.H. Gardner, A. Miltz, Evaluation of zinc oxide sorbents in a pilot-scale transport reactor: sulfidation kinetics and reactor modeling, Ind. Eng. Chem. Res. 43 (2004) 1235.

[8] Z. Hu, G. Oskam, P.C. Searson, Influence of solvent on the growth of ZnO nanoparticles, J. Colloid Interface Sci. 263 (2003) 454.

[9] E.A. Meulenkamp, Synthesis, growth of ZnO nanoparticles, J. Phys. Chem. B 102 (1998) 5566.

[10] S. Monticone, R. Tufeu, A.V. Kanaev, Complex nature of the UV and visible fluorescence of colloidal ZnO nanoparticles, J. Phys. Chem. B 102 (1990) 2854.

[11] D. Mondelaers, G. Vanhoyland, H. Van den Rul, J. D'Haen, M.K. Van Bael, J. Mullens, L.C. Van Poucke, Synthesis of ZnO nanopowder via an aqueous acetate–citrate gelation method, Mater. Res. Bull. 37 (2002) 901.

[12] M.S. Tokumoto, V. Brios, C.V. Santilli, S.H. Pulcinelli, Preparation of ZnO nanoparticles: structural study of the molecular precursor, J. Sol–Gel Sci. Technol. 26 (2003) 547.

[13] L.C. Damonte, L.A. Mendoza Zélis, B. Marí Soucase, M.A. Hernández Fenollosa, Nanoparticles of ZnO obtained by mechanical milling, Powder Technol. 148 (2004) 15.

[14] J.H. Kim, W.C. Choi, H.Y. Kim, Y. Kang, Y.-K. Park, Preparation of mono-dispersed mixed metal oxide microhollow spheres by homogeneous precipitation in a microprecipitator, Powder Technol. 153 (2005) 166.

[15] K. Okuyama, I. Wuled Lenggoro, Preparation of nanoparticles via spray route, Chem. Eng. Sci. 58 (2003) 537.

[16] M.L. Kahn, M. Monge, V. Collière, F. Senocq, A. Maisonnat, B. Chaudret, Size and shape control of crystalline zinc oxide nanoparticles: a new organometallic synthetic method, Adv. Funct. Mater. 15 (2005) 458.

[17] F. Rataboul, C. Nayral, M.J. Casanove, A. Maisonnat, B. Chaudret, Synthesis and characterization of monodisperse zinc and zinc oxide nanoparticles from the organometallic precursor [$Zn(C_6H_{11})_2$], J. Organomet. Chem. 643–644 (2002) 307.

[18] R. Viswanathan, G.D. Lilly, W.F. Gale, R.B. Gupta, Formation of zinc oxide–titanium dioxide composite nanoparticles in supercritical water, Ind. Eng. Chem. Res. 42 (2003) 5535.

[19] T. Sato, T. Tanigaki, H. Suzuki, Y. Saito, O. Kido, Y. Kimura, C. Kaito, A. Takeda, S. Kaneko, Structure and optical spectrum of ZnO nanoparticles produced in RF plasma, J. Cryst. Growth 255 (2003) 313.

[20] J. Wang, L. Gao, Synthesis, characterization of ZnO nanoparticles assembled in one-dimensional order, Inorg. Chem. Commun. 6 (2003) 877.

[21] W. Yu, X. Li, X. Gao, Catalytic Synthesis, structural characteristics of high-quality tetrapod-like ZnO nanocrystals by a modified vapor transport process, Cryst. Growth Des. 5 (2005) 151.

[22] Y.W. Koh, M. Lin, C.K. Tan, Y.L. Foo, K.P. Loh, Self-assembly and selected area growth of zinc oxide nanorods on any surface promoted by an aluminum precoat, J. Phys. Chem. B 108 (2004) 11419–11425.

[23] M. Singhal, V. Chhabra, P. Kang, D.O. Shah, Synthesis of ZnO nanoparticles for varistors application using Zn-substituted aerosol of microemulsion, Mater. Res. Bull. 32 (1997) 239.

[24] S. Komarneni, M. Bruno, E. Mariani, Synthesis of ZnO with and without microwaves, Mater. Res. Bull. 35 (2000) 1843.

[25] H. Zhang, D. Yang, Y. Ji, X. Ma, J. Xu, D. Que, Low temperature synthesis of flowerlike ZnO nanostructures by cetyltrimethylammonium bromide-assisted hydrothermal process, J. Phys. Chem. B 108 (2004) 3955.

[26] Z.R. Dai, Z.W. Pan, Z.L. Wang, Novel nanostructures of functional oxides synthesized by thermal evaporation, Adv. Funct. Mater. 13 (2003) 9.

[27] W. Ao, J. Li, H. Yang, X. Zeng, X. Ma, Mechanochemical synthesis of zinc oxide nanocrystalline, Powder Technol. 168 (2006) 148.

[28] A.K. Singh, Synthesis characterization electrical and sensing properties of ZnO nanoparticles, Adv. Powder Technol. 21 (2010) 609.

[29] A.K. Singh, V. Viswanath, V.C. Janu, Synthesis, effect of capping agents, structural, optical and photoluminescence properties of ZnO nanoparticles, J. Lumin. 129 (2009) 874.

[30] Z. Wang, X.F. Qian, J. Yin, Z.K. Zhu, Large-scale fabrication of tower-like, flower-like, and tube-like ZnO arrays by a simple chemical solution route, Langmuir 20 (2004) 3441–3448.

[31] H.L. Cao, X.F. Qian, Q. Gong, W.M. Du, X.D. Ma, Z.K. Zhu, Shape- and size-controlled synthesis of nanometre ZnO from a simple solution route at room temperature, Nanotechnology 17 (2006) 3632.

[32] M.T. Pope, A. Müller, Polyoxometalate Chemistry: From Topology via Self-Assembly to Applications, Kluwer, Dordrecht, The Netherlands, 2001.

[33] C.M. Teague, X. Li, M.E. Biggin, L. Lee, J. Kim, A.A. Gewirth, Vibrational spectroscopy of a Keggin polyoxometalate on metal electrode surfaces, J. Phys. Chem. B 108 (2004) 1974.

[34] A. Ayati, A. Ahmadpour, F.F. Bamoharram, M.M. Heravi, H. Rashidi, Photocatalytic synthesis of gold nanoparticles using preyssler acid and their photocatalytic activity, Chin. J. Catal. 32 (2011) 978.

[35] A. Ayati, A. Ahmadpour, F.F. Bamoharram, M.M. Heravi, H. Rashidi, B. Tanhaei, A new photocatalyst for preparation of silver nanoparticles and their photcatalysis of the decolorization of methyl orange, J. Nanostruct. Chem. 2 (2011) 15.

[36] F.F. Bamoharram, A. Ahmadpour, M.M. Heravi, A. Ayati, H. Rashidi, B. Tanhaei, Recent advances in application of polyoxometalates for the synthesis of nanoparticles, Synth. React. Inorg. Met. 42 (2012) 209.

[37] B. Keita, I.-M. Mbomekalle, L. Nadjo, C. Haut, Tuning the formal potentials of new VIV-substituted Dawson-type polyoxometalates for facile synthesis of metal nanoparticles, Electrochem. Commun. 6 (2004) 987.

[38] A. Troupis, A. Hiskia, E. Papaconstantinou, Synthesis of metal nanoparticles by using polyoxometalates as photocatalysts and stabilizers, Angew. Chem. Int. Ed. 41 (2002) 1911.

[39] S. Fardad, R. Massudi, Environment effect on structure, size control and stability of Zn and ZnO nanoparticles, in: Proc. 7th IEEE International Conference on Nanotechnology (IEEE-NANO 2007), Hong Kong, 2007.

[40] M. Wang, S.H. Hahn, J.S. Kim, J.S. Chung, E.J. Kim, K.K. Koo, Solvent-controlled crystallization of zinc oxide nano(micro)disks, J. Cryst. Growth 310 (2008) 1213–1219.

[41] B.D. Cullity, Elements of X-ray Diffraction, Reading, MA, 1978.

[42] S.K. Kulkarni, Nanotechnology: Principles and Practices, Capital Publishing Company, 2007.

[43] R. Hong, T. Pan, J. Qian, H. Li, Synthesis and surface modification of ZnO nanoparticles, Chem. Eng. J. 119 (2006) 71–81.

[44] Q. Li, E. Wang, S. Li, C. Wang, C. Tian, G. Sun, J. Gu, R. Xu, Template-free polyoxometalate-assisted synthesis for ZnO hollow spheres, J. Solid State Chem. 182 (2009) 1149–1155.

[45] Q. Ahsanulhaq, S.H. Kim, J.H. Kim, Y.B. Hahn, Structural properties and growth mechanism of flower-like ZnO structures obtained by simple solution method, Mater. Res. Bull. 43 (2008) 3483.

[46] G.H. Du, Y.Q. Yang, T.B. Li, B.S. Xu, Preparation of polymorphic ZnO with strong orange luminescence, J. Mater. Sci. Lett. 45 (2010) 1464.

[47] K.H. Tam, C.K. Cheung, Y.H. Leung, A.B. Djurišić, C.C. Ling, C.D. Beling, S. Fung, W.M. Kwok, W.K. Chan, D.L. Phillips, L. Ding, W.K. Ge, Defects in ZnO nanorods prepared by a hydrothermal method, J. Phys. Chem. B 110 (2006) 20865.

[48] M. Chakrabarti, S. Das, K.R. Chakrabarti, D. Sanyal, A. Chakrabarti, Room temperature optical and magnetic properties of polyvinylpyrrolidone capped ZnO nanoparticles, Mater. Charact. 60 (2009) 1014–1019.